

10

MICROWAVE PROPERTIES OF CHIRAL COMPOSITES

V. K. Varadan, Y. Ma, and V. V. Varadan

10.1 Introduction

10.2 Constitutive and Wave Equations For a Chiral Medium
10.3 Scattering From a Single Chiral Particle (T-Matrix)

10.4 Multiple Scattering Formulation

10.5 Results and Discussion

Acknowledgments

References

10.1 Introduction

It is well known that when a wave propagates through a medium containing dispersed particles, the entrained energy (intensity) is redistributed in various directions by scattering and absorbed by intrinsic absorption mechanisms, if any. By appropriately controlling the host and inclusion properties, as well as the geometry and distribution of the inclusion phase, it is possible to increase or decrease the scattering and absorption of energy in a composite medium. The selection of the inclusion phase is not an easy task and is application dependent.

From scattering theory, it is known generally that the larger the mismatch in physical properties between particles and their embedding medium, the larger is the scattering. Besides, the use of highly lossy materials can always attain the goal of high insertion loss and/or low reflection due to the high impedance mismatch. Despite considerable work reported in the past, prediction using correct theories of wave attenuation in various particulate media as well as artifacts, made to increase attenuation, is still challenging both the scientific and industrial communities. Significant applications include microwave com-

munication, laser propagation in atmosphere, and aerospace advanced materials.

In this chapter, we examine the effects of chirality (known as the optical activity in the optical literature [Bohren, 1974]) on the propagation of electromagnetic waves through a nonchiral medium containing randomly distributed particles made of a chiral material. The motive for this study is that the chirality of the inclusion phase can enhance scattering and absorption of electromagnetic waves. In what follows, the term chiral particle is used to denote the innate chirality of the inclusion material, not its shape which can be arbitrary. The introduction of chirality into mainstream electromagnetic theory is due to Bohren [1974] because there is no reason why chiral effects cannot exist at millimeter or microwave frequencies [Post, 1962; Jaggard, 1979]. Later investigation [Lakhtakia et al., 1985] has shown that a single, lossy, dielectric, chiral particle may scatter and/or absorb more electromagnetic energy than its nonchiral counterpart and the shape of the chiral particle could also play an important role in this energy dissipation game. Worthy notice is that wave absorbing composites made of chiral materials can be lighter and more flexible when compared with regular lossy dielectric and ferromagnetic ones.

When particles are dispersed in a host medium to form a composite, depending on the volume fraction of particles, single or multiple scattering effects may be dominant. Multiple scattering effects cannot be ignored when the concentration of particles is considerable. While these effects are known and shown for various dense systems [Varadan et al., 1983, 1985], they have never been investigated for chiral composites.

In this theoretical investigation, the chiral particles are spherical and have a uniform size distribution. Although these assumptions are not very restrictive to the multiple scattering formalism, the simpler model is able to show simply the effect due to the chirality, unshadowed by shape or size factors. The embedding medium also contributes to the attenuation, but here we focus attention on the inclusion phase. Therefore, inclusions and the matrix both made of chiral materials will not be considered here, though that they may enhance the attenuation further.

To cast the scattering response of a single chiral particle into the multiple scattering formalism, a T-matrix, which is a scattering transfer function, has been modified to include the chiral properties

[Lakhtakia et al., 1985]. An incident linearly polarized wave field will give rise to the right-circularly (RCP) and left-circularly (LCP) polarized fields inside the chiral particle and both fields propagate with different velocities. This complexities, not encountered in dielectric scatterers, do not generate any specific difficulties in the multiple scattering formulation used here if the effective medium is assumed to be nonchiral (or strictly speaking, weakly chiral). The reason is that, under this assumption, the propagation constant is independent of the field polarization state. Although a rigorous (and is currently under investigation) multiple scattering formalism needs to be introduced when the effective medium is chiral, at least in the low frequency regime, using the Bruggeman and the Maxwell-Garnett Approximations [Ward, 1988], we derive and present the dispersion equation for the composite medium which is effectively chiral.

In multiple scattering theory, because of the large population density of scatterers, it is essential to consider their relative positions; a detailed knowledge of the positional distribution of the scatterers is needed. This entails a consideration of inter-body forces as in the many body problem of statistical mechanics. At a minimum, the pair correlation function is required in analyzing the problem. It is well known that the Monte Carlo simulation method has yielded superior numerical results for the radial distribution function of densely distributed hard spheres [Barker and Henderson, 1971]. Therefore it is incorporated into computations of the effective attenuation rate in studying electromagnetic wave propagation through randomly distributed chiral spheres.

The plan of the paper is as follows. In Section 10.2 the constitutive properties and the governing field equations for chiral media are examined. Scattering from a single chiral sphere in a nonchiral medium and its associated T-matrix are introduced in Section 10.3. In the same section, the low frequency expansions of the scattered field coefficients from a single chiral sphere are also presented. In Section 10.4, the T-matrix is employed in the multiple scattering formalism to obtain a dispersion equation for the chiral composite materials which are made by dispersing a large number chiral particles in a nonchiral matrix. The low frequency expressions of the dispersion equation using the Bruggeman approximation as well as the Maxwell-Garnett approximation are also given in this section. Finally, computed results of microwave properties of chiral composite materials, through solving

the dispersion equation numerically, are presented.

10.2 Constitutive and Wave Equations for a Chiral Medium

Consider a region V occupied by an isotropic chiral medium in which the constitutive relations

$$\mathbf{D} = \epsilon_c \mathbf{E} + \beta_c \epsilon_c \nabla \times \mathbf{E}, \quad \mathbf{B} = \mu_c \mathbf{H} + \beta_c \mu_c \nabla \times \mathbf{H} \quad (1)$$

hold [Bohren, 1974]. Use is now made of the regular Maxwell's equations along with (1) to obtain the relation

$$\nabla^2 \begin{bmatrix} \mathbf{E} \\ \mathbf{H} \end{bmatrix} = -[K]^2 \begin{bmatrix} \mathbf{E} \\ \mathbf{H} \end{bmatrix}, \quad \nabla \times \begin{bmatrix} \mathbf{E} \\ \mathbf{H} \end{bmatrix} = [K_c] \begin{bmatrix} \mathbf{E} \\ \mathbf{H} \end{bmatrix}, \quad \nabla \cdot \begin{bmatrix} \mathbf{E} \\ \mathbf{H} \end{bmatrix} = \begin{bmatrix} 0 \\ 0 \end{bmatrix} \quad (2)$$

where the matrix

$$[K_c] = [1 - (k_c \beta_c)^2]^{-1} \begin{bmatrix} k_c^2 \beta_c & i\omega \mu_c \\ -i\omega \epsilon_c & k_c^2 \beta_c \end{bmatrix} \quad (3)$$

with $k_c = \omega \{\mu_c \epsilon_c\}^{1/2}$, and an $\exp[-i\omega t]$ time dependence has been assumed. Following Bohren [1974], the EM field is transformed to

$$\begin{bmatrix} \mathbf{E} \\ \mathbf{H} \end{bmatrix} = [A_c] \begin{bmatrix} \mathbf{Q}_L \\ \mathbf{Q}_R \end{bmatrix} \quad (4)$$

where the left- (LCP) and the right- (RCP) circularly polarized fields, \mathbf{Q}_L and \mathbf{Q}_R , respectively, must satisfy the conditions

$$\{\nabla^2 + k_L^2\} \mathbf{Q}_L = 0; \quad \{\nabla^2 + k_R^2\} \mathbf{Q}_R = 0 \quad (5)$$

along with the auxiliary conditions

$$\nabla \times \mathbf{Q}_L = k_L \mathbf{Q}_L; \quad \nabla \cdot \mathbf{Q}_L = 0 \quad (6a)$$

and

$$\nabla \times \mathbf{Q}_R = -k_R \mathbf{Q}_R; \quad \nabla \cdot \mathbf{Q}_R = 0 \quad (6b)$$

In these equations, the matrix

$$[A_c] = \begin{bmatrix} 1 & a_R \\ a_L & 1 \end{bmatrix} \quad (7a)$$

while,

$$k_L = k_c / \{1 - k_c \beta_c\}; \quad a_L = -i(\epsilon_c / \mu_c)^{1/2} \quad (7b)$$

and

$$k_R = k_c / \{1 + k_c \beta_c\}; \quad a_R = -i(\epsilon_c / \mu_c)^{-1/2} \quad (7c)$$

10.3 Scattering from a Single Chiral Particle (T-matrix)

To cast the scattering response of a single chiral sphere into the multiple scattering formalism, a T-matrix, which is a scattering transfer function used in the formalism, has to be modified to include the specific chiral properties [Lakhtakia et al., 1985]. The overall goal in using the T-matrix procedure is to determine the fields induced inside a permeable scatterer as well as the fields scattered by it when it is illuminated by an incident electromagnetic field. The relative ease of computation offered by the T-matrix method has been discussed elsewhere [Waterman, 1969; Barber and Yeh, 1975; Varadan et al., 1980, 1988; Tsang et al., 1985].

Consider a chiral sphere embedded in a nonchiral host medium excited by a linearly polarized plane EM wave. The incident, scattered and the induced (field inside the scatterer) fields are generally expanded in vector spherical harmonics M_n and N_n [Morse and Feshbach, 1953].

The incident electric and magnetic fields E^o and H^o can be expressed, respectively, as

$$E^o = \sum i^n [(2n+1)/n(n+1)] [M_{o1n(1)}(kr) - iN_{e1n(1)}(kr)] \quad (8a)$$

$$H^o = (-k/\mu\omega) \sum i^n [(2n+1)/n(n+1)] [M_{e1n(1)}(kr) + iN_{o1n(1)}(kr)] \quad (8b)$$

which are independent of the properties of scatterers. In Eqs. (8a) and (8b), k , ϵ and μ refer to the (nonchiral) host medium. Attention must be paid to both the scattered and the induced fields because only circularly polarized fields can exist in a chiral medium. The fields inside the scatterer can be expressed through

$$Q_L = \sum i^n [(2n+1)/n(n+1)] \{ f_n [M_{o1n(1)}(k_L r) + N_{o1n(1)}(k_L r)] + g_n [M_{e1n(1)}(k_L r) + N_{e1n(1)}(k_L r)] \}$$

$$+ \mathbf{N}_{e1n^{(1)}}(k_L \mathbf{r})] \} \quad (9a)$$

$$\begin{aligned} \mathbf{Q}_R = \sum i^n [(2n+1)/n(n+1)] \{ & p_n [\mathbf{M}_{o1n^{(1)}}(k_R \mathbf{r}) \\ & + \mathbf{N}_{o1n^{(1)}}(k_R \mathbf{r})] + w_n [\mathbf{M}_{e1n^{(1)}}(k_R \mathbf{r}) \\ & + \mathbf{N}_{e1n^{(1)}}(k_R \mathbf{r})] \} \end{aligned} \quad (9b)$$

The scattered field is circularly polarized and propagates with the speed ω/k . Again, it can be expanded in terms of vector spherical harmonics which satisfy the radiation condition at infinity, Thus,

$$\begin{aligned} \mathbf{E}^s = \sum i^n [(2n+1)/n(n+1)] \{ & a_n \mathbf{M}_{o1n^{(s)}}(k \mathbf{r}) \\ & - ib_n \mathbf{N}_{e1n^{(s)}}(k \mathbf{r}) + c_n \mathbf{M}_{e1n^{(s)}}(k \mathbf{r}) \\ & - id_n \mathbf{N}_{o1n^{(s)}}(k \mathbf{r}) \} \end{aligned} \quad (10a)$$

$$\begin{aligned} \mathbf{H}^s = \sum i^n [(2n+1)/n(n+1)] \{ & b_n \mathbf{M}_{e1n^{(s)}}(k \mathbf{r}) \\ & + ia_n \mathbf{N}_{o1n^{(s)}}(k \mathbf{r}) + d_n \mathbf{M}_{o1n^{(s)}}(k \mathbf{r}) \\ & + ic_n \mathbf{N}_{e1n^{(s)}}(k \mathbf{r}) \} \end{aligned} \quad (10b)$$

The boundary conditions for the problem are the same as those for dielectric spheres which require both the tangential components of the \mathbf{E} and \mathbf{H} fields to be continuous at the surface of the scatterer. However, due to the chirality of the scatterer, 8 unknowns, instead of the usual 4 for a dielectric sphere, are introduced into the equations. We skip the details [Bohren, 1974] and show only the results for the scattered field coefficients a_n , b_n , c_n and d_n :

$$\begin{aligned} a_n = -[W_n(L)A_n(R) + W_n(R)A_n(L)]/[W_n(L)V_n(R) \\ + W_n(R)V_n(L)] \end{aligned} \quad (11a)$$

$$\begin{aligned} b_n = -[B_n(L)V_n(R) + B_n(R)V_n(L)]/[W_n(L)V_n(R) \\ + W_n(R)V_n(L)] \end{aligned} \quad (11b)$$

$$\begin{aligned} c_n = -[W_n(L)B_n(R) - W_n(R)B_n(L)]/[W_n(L)V_n(R) \\ + W_n(R)V_n(L)] \end{aligned} \quad (11c)$$

$$d_n = -c_n \quad (11d)$$

where,

$$W_n(J) = m\phi_n(m_J x)\zeta'_n(x) - \phi'_n(m_J x)\zeta_n(x) \quad (12a)$$

$$V_n(J) = -\phi_n(m_J x)\zeta'_n(x) - m\phi'_n(m_J x)\zeta_n(x) \quad (12b)$$

$$A_n(J) = \phi_n(m_J x)\phi'_n(x) - m\phi'_n(m_J x)\phi_n(x) \quad (12c)$$

$$B_n(J) = m\phi_n(m_J x)\phi'_n(x) - \phi'_n(m_J x)\phi_n(x) \quad (12d)$$

J is either L or R and $x = ka$. The prime denotes differentiation with respect to the argument; $\phi_n(z) = zj_n(z)$, $\zeta_n(z) = zh_n(z)$; while j_n and h_n are the spherical Bessel and Hankel functions, respectively. The relative refractive indices, $m_L = k_L/k$, $m_R = k_R/k$ and $m = (\epsilon_c\mu/\epsilon\mu_c)^{1/2}$.

In terms of the T-matrix, which relates the unknown scattered field coefficients to the known incident field coefficients [Varadan and Varadan, 1980], a_n, b_n, c_n and d_n are simply its diagonal elements and for a spherical scatterer, these are the only nonvanishing elements in the T-matrix. In addition, if the scatterer loses its chirality, the present procedures degenerate into the well known Mie solution.

In the low frequency regime, i.e., when $ka, k_L a$ and $k_R a \ll 1$, the expansions of the Bessel and Hankel functions in powers of their arguments are truncated so that only terms up to the order $O[(ka)^3]$ are considered. Therefore, from (11) and (12) we obtain

$$a_1 = (i2x^3/3)[(mm_L - 1)(2m + m_R) + (mm_R - 1)(2m + m_L)]/\Delta \quad (13a)$$

$$b_1 = (i2x^3/3)[(mm_L + 2)(m_R - m) + (mm_R + 2)(m_L - m)]/\Delta \quad (13b)$$

$$c_1 = (i2x^3/3)[(mm_L + 2)(mm_R - 1) - (mm_R + 2)(mm_L - 1)]/\Delta \quad (13c)$$

$$d_1 = -c_1 \quad (13d)$$

$$\Delta = (-9m_L m_R)[(mm_L + 2)(2m + m_R) + (mm_R + 2)(2m + m_L)] \quad (13e)$$

10.4 Multiple Scattering Formulation

In this section, the average field in the random medium is written as a partial summation of a multiple scattering series. By assuming that the average field is a plane wave with an effective wave number K , the resulting dispersion equation is obtained. Only the most important details that lead to the dispersion equation involving the pair correlation are presented and for all intermediate steps, we refer the reader to [Varadan et al., 1979]. Vector notation is dispensed with, but the formalism is applicable to the electromagnetic field satisfying the vector Helmholtz equation.

Let the nonchiral medium contain N randomly distributed spherical scatterers in a volume V such that $N \rightarrow \infty, V \rightarrow \infty$ but $n_0 = N/V$ the number density of scatterers is finite. Let u, u^o, u_i^e, u_i^s be respectively the total field; the incident field; the field exciting the i th scatterer; and the field which is in turn scattered by the i th scatterer.

Let $\text{Re}\phi_n$ and $\text{Ou}\phi_n$ denote the basis of orthogonal functions which are regular at the origin and outgoing at infinity which are, respectively, appropriate for expanding the field which excites a scatterer and that which it scatters which in turn must satisfy outgoing or radiation conditions. Thus, we can write the following set of self-consistent equations:

$$u = u^o + \sum u_i^s \quad (14a)$$

$$u^o = \sum a_n^i \text{Re}\phi_n(\mathbf{r} - \mathbf{r}_i) \quad (14b)$$

$$u_i^e = \sum \alpha_n^i \text{Re}\phi_n(\mathbf{r} - \mathbf{r}_i); b < |\mathbf{r} - \mathbf{r}_i| < 2b \quad (14c)$$

$$u_i^s = \sum f_n^i \text{Ou}\phi_n(\mathbf{r} - \mathbf{r}_i); |\mathbf{r} - \mathbf{r}_i| > b \quad (14d)$$

where α_n^i and f_n^i are unknown expansion coefficients. We observe here that b is the radius of the sphere circumscribing the scatterer and that all expansions are with respect to a coordinate origin located in a particular scatterer.

The T-matrix by definition simply relates the expansion coefficients of u_i^e and u_i^s provided $u_i^e + u_i^s$ is the total field which is consistent with the definitions given above. Thus, [Varadan and Varadan, 1980],

$$f_n^i = \sum T_{nn'} \alpha_{n'}^i \quad (15)$$

and the following addition theorem for the basis functions is invoked

$$\text{Ou}\phi_n(\mathbf{r} - \mathbf{r}_j) = \sum \sigma_{nn'}(\mathbf{r}_i - \mathbf{r}_j) \text{Re}\phi_{n'}(\mathbf{r} - \mathbf{r}_i) \quad (16)$$

Substituting (14b,c,d), (15) and (16) in (14a), and using the orthogonality of the basis functions we obtain

$$\alpha^i = a^i + \sum_{j \neq i} T^j \sigma(\mathbf{r}_i - \mathbf{r}_j) \alpha^j \quad (17)$$

This is a set of coupled algebraic equations for the exciting field coefficients which can be iterated and leads to a multiple scattering series.

For randomly distributed scatterers, an ensemble average can be performed on (17) leading to

$$\langle \alpha^i \rangle_i = a^i + \langle \sigma(\mathbf{r}_i - \mathbf{r}_j) T^j \langle \alpha^j \rangle_j \rangle_i \quad (18)$$

where angle brackets and $ij\dots$ denotes a conditional average and (18) when iterated is an infinite hierarchy involving higher and higher conditional expectations of the exciting field coefficients. In actual engineering applications, a knowledge of higher order correlation functions is difficult to obtain, and usually the hierarchy is truncated so that at most only the two body positional correlation function is required.

To achieve this simplification the quasi-crystalline approximation (QCA), first introduced by Lax [1952] is invoked, which is stated as

$$\langle \alpha^j \rangle_{ij} \approx \langle \alpha^j \rangle_j \quad (19)$$

Then, (18) simplifies to

$$\langle \alpha^i \rangle_i = a^i + \langle \sigma(\mathbf{r}_i - \mathbf{r}_j) T^j \langle \alpha^j \rangle_j \rangle_i \quad (20)$$

an integral equation for $\langle \alpha^i \rangle_i$ which in principle can be solved. We observe that the ensemble average in (20) only requires $p(\mathbf{r}_j | \mathbf{r}_i)$, the joint probability distribution function. In particular, the homogeneous solution of (20) leads to a dispersion equation for the effective medium in the quasi-crystalline approximation. Defining the spatial Fourier transform of $\langle \alpha^i \rangle_i$ as

$$\langle \alpha^i \rangle_i = \int e^{i\mathbf{K} \cdot \mathbf{r}_i} X^i(\mathbf{K}) d\mathbf{K} \quad (21)$$

and substituting in (20), we obtain for the homogeneous solution

$$X^i(\mathbf{K}) = \sum_{j \neq i} \int \sigma(\mathbf{r}_i - \mathbf{r}_j) T^j p(\mathbf{r}_j | \mathbf{r}_i) \times e^{i\mathbf{K} \cdot (\mathbf{r}_i - \mathbf{r}_j)} d\mathbf{r}_j X^j(\mathbf{K}) \quad (22)$$

Thus for a nontrivial solution to $\langle \alpha^i \rangle_i$, we require [Varadan et al., 1985]

$$|I - \sum_{j \neq i} \int \sigma(\mathbf{r}_i - \mathbf{r}_j) T^j p(\mathbf{r}_j | \mathbf{r}_i) e^{i\mathbf{K} \cdot (\mathbf{r}_i - \mathbf{r}_j)} d\mathbf{r}_j| = 0 \quad (23)$$

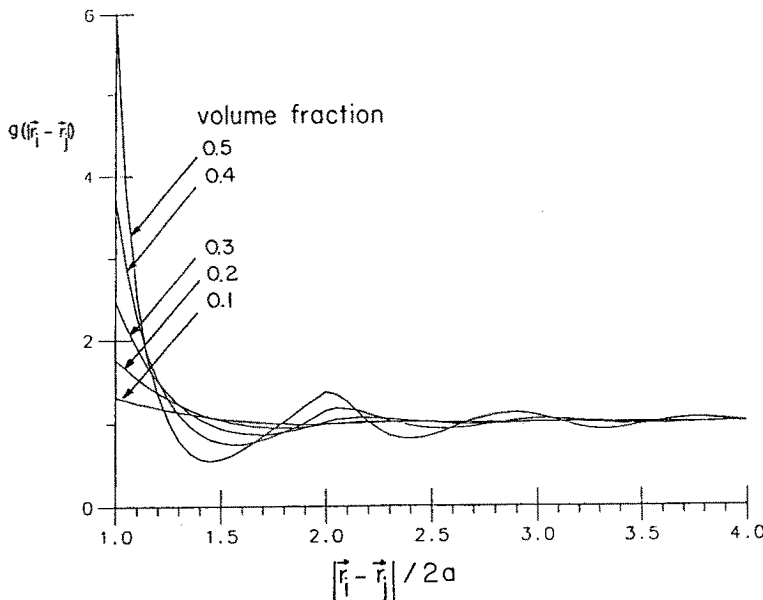


Figure 10.1 Radial distribution function vs. interparticle distance for different volume fraction.

In (22) and (23), $p(\mathbf{r}_j|\mathbf{r}_i)$ is the joint probability distribution function. For spherical statistics,

$$p(\mathbf{r}_j|\mathbf{r}_i) = \begin{cases} 0; & |\mathbf{r}_i - \mathbf{r}_j| < 2b \\ g(|\mathbf{r}_i - \mathbf{r}_j|)/V; & |\mathbf{r}_i - \mathbf{r}_j| > 2b \end{cases} \quad (24)$$

where we have assumed that the scatterers are impenetrable with a minimum separation between the centers, and $2b$ is the diameter of the circumscribing sphere. For spherical scatterers, the joint probability distribution depends only on the interparticle distance and not on the orientation of the vector joining the centers. The function $g(|\mathbf{r}_i - \mathbf{r}_j|)$ is called the radial distribution function. In Fig. 10.1, different values of the radial distribution function for different volume fractions are plotted against the normalized radial distance using the Monte Carlo technique [Barker and Henderson, 1971].

Equation (23) is known as the dispersion equation of the effective medium. By effective medium we mean that a microscopically discrete random medium, in which a wave propagates, can be replaced by a macroscopically homogeneous medium characterized by an effective wavenumber K . The effective wavenumber which is a complex propa-

gation constant can be used to derive the effective properties, e.g., effective dielectric constants ϵ_{eff} via $\epsilon_{\text{eff}}\mu_0 = K^2/\omega^2$, of the nonmagnetic composite medium. Although randomly distributed inclusion phases (chiral spheres) undergo multiple scattering, an average wave, which is a plane wave propagating in this effective medium along the incident plane wave direction, does not suffer further scattering. However, its velocity and amplitude now are determined by the new propagation constant K .

The dispersion is a determinantal equation. Its roots can be solved numerically to yield the values of the effective wavenumber, $K = K_1 + iK_2$ as a function of the frequency via k , the size and properties of the scatterer via the T-matrix and the statistics of the distribution via the joint probability distribution function. The real part K_1 describes the phase velocity while the imaginary part K_2 gives the attenuation of the amplitude of the average wave in the effective medium.

Dispersion Equations - Low Frequency Expansions

The multiple scattering formalism required to obtain the dispersion equation in the microwave frequency range ($ka > 1$) is shown for an effectively nonchiral composite medium. In order to handle an effective medium which is chiral, the present multiple scattering formalism needs to be modified and is currently under investigation. However, in the low frequency regime, i.e., $ka \ll 1$, the Bruggeman approximation (BA) as well as the Maxwell-Garnett approximation (MGA) may be used instead to study the effective medium which is either nonchiral or chiral.

In the Bruggeman approximation, the two components (inclusions and matrix) of the composite are treated in an equivalent manner, whereas in the Maxwell-Garnett approximation, the grains of one component are considered to be embedded in the matrix of the other component. Consequently, the BA has the property of invariance with respect to a change in the roles of matrix and inclusions. However, in the MGA one needs to make a choice as to which component is the matrix phase and which one is the inclusion phase. Nevertheless, both the BA and the MGA become exact for a composite having one component and containing only a small fraction of the other component. Details for the BA and the MGA as applied for the present purposes are given by Khebir [1986] and only the dispersion equations are repeated here.

The Nonchiral Effective Medium - BA

Assuming that an LCP plane wave travels through an effective nonchiral medium, it can be shown that

$$\begin{aligned} \sum c_n \left[(\epsilon_n + 2\epsilon_{\text{eff}})^{-1} \left\{ -2i \left[\epsilon_n - \epsilon_{\text{eff}} - k_L a (\epsilon_{\text{eff}})^{1/2} \epsilon_n (\beta/a) \right] / 3 \right\} \right. \\ + [\epsilon_{\text{eff}} (2\epsilon_{\text{eff}} + \epsilon_n)^2]^{-1} \times \{ (k_L a)^2 (i\epsilon_{\text{eff}}/45) [40\epsilon_{\text{eff}}^3 - 72\epsilon_{\text{eff}}^2 \epsilon_n \\ + (\epsilon_n + 2\epsilon_{\text{eff}}) \{-2\epsilon_{\text{eff}}^2 + 10\epsilon_{\text{eff}} \epsilon_n - 8\epsilon_n^2 + 170\epsilon_{\text{eff}} \epsilon_n (\beta/a)^2 - 150\epsilon_n^2 \\ (\beta/a)^2\}] + 24\epsilon_{\text{eff}} \epsilon_n^2 + 8\epsilon_n^3 - 340\epsilon_{\text{eff}}^2 \epsilon_n (\beta/a)^2 + 190\epsilon_{\text{eff}} \epsilon_n^2 (\beta/a)^2 \\ + 150\epsilon_n^3 (\beta/a)^2 \} + [\epsilon_{\text{eff}} (\epsilon_n + 2\epsilon_{\text{eff}})]^{-1} (k_L a)^2 (i\epsilon_{\text{eff}}/45) \times [-\epsilon_{\text{eff}}^2 \\ \left. + \epsilon_{\text{eff}} \epsilon_n + \epsilon_n^2 + 20\epsilon_{\text{eff}} \epsilon_n (\beta/a)^2] \right] = 0 \end{aligned} \quad (25)$$

where ϵ_{eff} is the effective permittivity of the nonchiral effective medium for LCP plane wave propagation. For RCP plane wave propagation, the dispersion equation remains the same except that the wavenumber k_L is replaced by k_R .

In the above and subsequent equations, the subscript $n = 1$ corresponds to the inclusion; hence, $c_1 = c$ (volume fraction of the chiral scatterers) and $\epsilon_1 = \epsilon_c$. The subscript $n = 2$ corresponds to the host; thus, $c_2 = 1 - c$ and $\epsilon_2 = \epsilon$.

The Chiral Effective Medium - BA

When the effective medium is supposed to be effectively chiral, the Bruggeman approximation leads to two polynomial equations.

$$\begin{aligned} \sum c_n \left[i[3(\epsilon_n + 2\epsilon_{\text{eff}})]^{-1} \{ \epsilon_n - \epsilon_{\text{eff}} + 2(\epsilon_n \beta_{\text{eff}}/a + \epsilon_n \beta_n/a \right. \\ - 2\epsilon_{\text{eff}} \beta_{\text{eff}}/a) k_L a \epsilon_{\text{eff}}^{1/2} + [30\epsilon_{\text{eff}} (\epsilon_n + 2\epsilon_{\text{eff}})]^{-1} [(\epsilon_n + 2\epsilon_{\text{eff}}) \{-7\epsilon_n^2 \\ - 150\epsilon_n^2 \beta_n^2/a^2 + 11\epsilon_n \epsilon_{\text{eff}} - 170\epsilon_n \epsilon_{\text{eff}} \beta_{\text{eff}}^2/a^2 + 160\epsilon_n \epsilon_{\text{eff}} \beta_{\text{eff}} \beta_n/a^2 \\ + 190\epsilon_n \epsilon_{\text{eff}} \beta_n^2/a^2 - 4\epsilon_{\text{eff}}^2 - 30\epsilon_{\text{eff}}^2 \beta_{\text{eff}}^2/a^2\} + 8\epsilon_n^3 + 150\epsilon_n^3 \beta_n^2/a^2 \\ + 24\epsilon_n^2 \epsilon_{\text{eff}} + 250\epsilon_n^2 \epsilon_{\text{eff}} \beta_{\text{eff}}^2/a^2 + 40\epsilon_n^2 \epsilon_{\text{eff}} \beta_{\text{eff}} \beta_n/a^2 + 190\epsilon_n^2 \epsilon_{\text{eff}} \beta_n^2/a^2 \\ - 72\epsilon_n \epsilon_{\text{eff}}^2 + 230\epsilon_n \epsilon_{\text{eff}}^2 \beta_{\text{eff}}^2/a^2 - 40\epsilon_n \epsilon_{\text{eff}}^2 \beta_{\text{eff}} \beta_n/a^2 - 340\epsilon_n \epsilon_{\text{eff}}^2 \beta_n^2/a^2 \\ \left. + 40\epsilon_{\text{eff}}^3 - 480\epsilon_{\text{eff}}^3 \beta_{\text{eff}}^2/a^2\} (k_L a)^2 \epsilon_{\text{eff}} \} \right] = 0 \end{aligned} \quad (26a)$$

and

$$\sum c_n \left[i[9(\epsilon_n + 2\epsilon_{\text{eff}})]^{-1} \{ \epsilon_n - 7\epsilon_{\text{eff}} - 2(\epsilon_n\beta_n/a - 10\epsilon_{\text{eff}}\beta_{\text{eff}}/a)k_L a \epsilon_{\text{eff}}^{1/2} \right. \\ + [30(\epsilon_n + 2\epsilon_{\text{eff}})]^{-1} [(\epsilon_n + 2\epsilon_{\text{eff}}) \{ -9\epsilon_n^2 - 150\epsilon_n^2\beta_n^2/a^2 + 111\epsilon_n\epsilon_{\text{eff}} \\ - 330\epsilon_n\epsilon_{\text{eff}}\beta_{\text{eff}}^2/a^2 + 240\epsilon_n\epsilon_{\text{eff}}\beta_{\text{eff}}\beta_n/a^2 + 1170\epsilon_n\epsilon_{\text{eff}}\beta_n^2/a^2 - 48\epsilon_{\text{eff}}^2 \\ + 510\epsilon_{\text{eff}}^2\beta_{\text{eff}}^2/a^2 \} + 8\epsilon_n^3 + 280\epsilon_{\text{eff}}^3 + 150\epsilon_n^3\beta_n^2/a^2 - 24\epsilon_n^2\epsilon_{\text{eff}} \\ + 250\epsilon_n^2\epsilon_{\text{eff}}\beta_{\text{eff}}^2/a^2 + 40\epsilon_n^2\epsilon_{\text{eff}}\beta_n\beta_{\text{eff}}/a^2 - 710\epsilon_n^2\epsilon_{\text{eff}}\beta_n^2/a^2 - 264\epsilon_n\epsilon_{\text{eff}}^2 \\ - 1270\epsilon_n\epsilon_{\text{eff}}^2\beta_{\text{eff}}^2/a^2 - 280\epsilon_n\epsilon_{\text{eff}}^2\beta_{\text{eff}}\beta_n/a^2 - 2380\epsilon_n\epsilon_{\text{eff}}^2\beta_n^2/a^2 \\ \left. - 3360\epsilon_{\text{eff}}^3\beta_{\text{eff}}^2/a^2 \} (k_L a)^2 \epsilon_{\text{eff}} \} \right] = 0 \quad (26b)$$

Since the host is nonchiral, $\beta_2 = 0$ while $\beta_1 = \beta_c$ in (26a, b). Equations (26a, b) have to be simultaneously solved using numerical techniques on a digital computer to obtain ϵ_{eff} and β_{eff} of the chiral effective medium.

The Maxwell-Garnett Approximation

Likewise, if chiral particles dispersed in a nonchiral medium is assumed to be chiral, the MGA also yields two equations which involve ϵ_{eff} and β_{eff} :

$$(-2i/3)[(\epsilon_{\text{eff}} - \epsilon)/(\epsilon_{\text{eff}} + 2\epsilon) - c(\epsilon_c - \epsilon)/(\epsilon_{\text{eff}} + 2\epsilon)] - k_L a(\epsilon)^{1/2} \\ [\epsilon_{\text{eff}}(\beta_{\text{eff}}/a) - c\epsilon_c(\beta_c/a) + (k_L a)^2(\epsilon i/45)\{\epsilon^{-1}(\epsilon_{\text{eff}} + 2\epsilon)^{-2}(40\epsilon^3 \\ - 72\epsilon^2\epsilon_{\text{eff}} + (\epsilon_{\text{eff}} + 2\epsilon)\{-2\epsilon^2 + 10\epsilon\epsilon_{\text{eff}} - 8\epsilon_{\text{eff}}^2 + 170\epsilon\epsilon_{\text{eff}}\beta_{\text{eff}}^2/a^2 \\ - 150\epsilon_{\text{eff}}^2\beta_{\text{eff}}^2/a^2\} + 24\epsilon\epsilon_{\text{eff}}^2 + 8\epsilon_{\text{eff}}^3 - 340\epsilon^2\epsilon_{\text{eff}}\beta_{\text{eff}}^2/a^2 \\ + 190\epsilon_{\text{eff}}^2\beta_{\text{eff}}^2/a^2 + 150\epsilon_{\text{eff}}^3\beta_{\text{eff}}^2/a^2\} - c\epsilon^{-1}(\epsilon_c + 2\epsilon)^{-2} \\ (40\epsilon^3 - 72\epsilon^2\epsilon_c + (\epsilon_c + 2\epsilon) \times \{-2\epsilon^2 + 10\epsilon\epsilon_c - 8\epsilon_c^2 + 170\epsilon\epsilon_c\beta_c^2/a^2 \\ - 150\epsilon_c^2\beta_c^2/a^2\} + 24\epsilon\epsilon_c^2 + 8\epsilon_c^3 - 340\epsilon^2\epsilon_c\beta_c^2/a^2 + 190\epsilon\epsilon_c^2\beta_c^2/a^2 \\ + 150\epsilon_c^2\beta_c^2/a^2) + \epsilon^{-1}(\epsilon_{\text{eff}} + 2\epsilon)(-\epsilon^2 + \epsilon\epsilon_{\text{eff}} + \epsilon_{\text{eff}}^2 + 20\epsilon\epsilon_{\text{eff}}\beta_{\text{eff}}^2/a^2) \\ - c\epsilon^{-1}(\epsilon_c + 2\epsilon) \times (-\epsilon^2 + \epsilon\epsilon_c + \epsilon_c^2 + 20\epsilon\epsilon_c\beta_c^2/a^2)\} = 0 \quad (27a)$$

and

$$(-2i/3)[(\epsilon_{\text{eff}} - \epsilon)/(\epsilon_{\text{eff}} + 2\epsilon) - c(\epsilon_c - \epsilon)/(\epsilon_{\text{eff}} + 2\epsilon)] + k_L a(\epsilon)^{1/2} \\ [\epsilon_{\text{eff}}(\beta_{\text{eff}}/a) - c\epsilon_c(\beta_c/a) + (k_L a)^2(\epsilon i/45)\{\epsilon^{-1}(\epsilon_{\text{eff}} + 2\epsilon)^{-2}$$

$$\begin{aligned}
 & (40\epsilon^3 - 72\epsilon^2\epsilon_{\text{eff}} + (\epsilon_{\text{eff}} + 2\epsilon)\{-2\epsilon^2 + 10\epsilon\epsilon_{\text{eff}} - 8\epsilon_{\text{eff}}^2 \\
 & + 170\epsilon\epsilon_{\text{eff}}\beta_{\text{eff}}^2/a^2 - 150\epsilon_{\text{eff}}^2\beta_{\text{eff}}^2/a^2\} + 24\epsilon\epsilon_{\text{eff}}^2 + 8\epsilon_{\text{eff}}^3 \\
 & - 340\epsilon^2\epsilon_{\text{eff}}\beta_{\text{eff}}^2/a^2 + 190\epsilon\epsilon_{\text{eff}}^2\beta_{\text{eff}}^2/a^2 + 150\epsilon_{\text{eff}}^3\beta_{\text{eff}}^2/a^2] \\
 & - c\epsilon^{-1}(\epsilon_c + 2\epsilon)^{-2}(40\epsilon^3 - 72\epsilon^2\epsilon_c + (\epsilon_c + 2\epsilon) \times \{-2\epsilon^2 \\
 & + 10\epsilon\epsilon_c - 8\epsilon_c^2 + 170\epsilon\epsilon_c\beta_c^2/a^2 - 150\epsilon_c^2\beta_c^2/a^2\} + 24\epsilon\epsilon_c^2 + 8\epsilon_c^3 \\
 & - 340\epsilon^2\epsilon_c\beta_c^2/a^2 + 190\epsilon\epsilon_c^2\beta_c^2/a^2 + 150\epsilon_c^3\beta_c^2/a^2) + \epsilon^{-1} \\
 & (\epsilon_{\text{eff}} + 2\epsilon)(-\epsilon^2 + \epsilon\epsilon_{\text{eff}} + \epsilon_{\text{eff}}^2 + 20\epsilon\epsilon_{\text{eff}}\beta_{\text{eff}}^2/a^2) - c\epsilon^{-1} \\
 & (\epsilon_c + 2\epsilon)(-\epsilon^2 + \epsilon\epsilon_c + \epsilon_c^2 + 20\epsilon\epsilon_c\beta_c^2/a^2)\} = 0
 \end{aligned} \tag{27b}$$

10.5 Results and Discussion

We have reported scattering and absorption characteristics of a single chiral object in an earlier paper [Lakhtakia et al., 1985]. In which the properties of the chiral object, ϵ_c , μ_c and β_c used there were adopted for this multiple scattering analysis. The chiral parameter $\beta_c = 10^{-4}\text{m}$ and $\mu_c = \mu_0$ were assumed to be frequency independent but need not be so. Nevertheless, the relative permittivity ϵ_c/ϵ_0 was chosen to be complex and frequency dependent with values listed in Table 10.1. The radius of the sphere was 0.2 mm and chiral particles were assumed suspended in free space. (We have observed elsewhere [Varadan et al., 1987] that the reflection of plane waves by a planar chiral plate, sitting upon a perfectly conducting substrate and having these properties of table 10.1, is almost uniformly less than 25% over a 50 - 300 GHz frequency range for incidence angles $\theta_0 \leq 30^\circ$. Should, however, $\beta_c = 0$, the reflection coefficients vary considerably and can have values up to $\approx 85\%$.) Although β_c is likely to be frequency dependent as well, in this study it is assumed to be constant. Since the kind of chiral scatterers envisioned here are yet not available, and their feasibility is to be devoutly hoped for, the value of β_c used in the preceding calculations is purely arbitrary. Proteins in the ultra-violet range usually have lower values, but one will have to wait measurements on possible chiral composites before any given value of β_c for non-molecular chiral properties in the GHz range can be estimated, because their chirality would be at the structural level rather than at the molecular level.

The real and imaginary parts of the effective wave number K , which is related to the phase velocity and attenuation in the effective

Frequency (GHz)	Real (ϵ_c / ϵ_0)	Imag(ϵ_c / ϵ_0)
60	17.4	0.435
70	15.8	0.395
80	15.7	0.314
90	15.56	0.156
100	14.74	0.0737
110	12.82	0.0641
120	10.8	0.054
130	9.9	0.0396
140	8.4	0.0336
150	7.91	0.0316
160	7.0	0.028

Table 10.1 Complex relative permittivity of the chiral scatterers (properties used in obtaining numerical results in Figs. 10.2 and 10.3).

medium, respectively, can be obtained by numerically solving the dispersion equation (22). In Fig. 10.2, the normalized phase velocity, i.e., real part of k/K , showed that even for a volume fraction $c = 5\%$ of chiral suspensions, the chirality of scatterers changed the dispersion pattern of the effective medium drastically. For the lossy dielectric sphere case ($\beta_c = 0$), the wave travelled with a more or less constant speed but it was not so for the chiral sphere case in which the phase velocity was highly frequency dependent and could be faster and slower than that of the nonchiral case.

As for the attenuation, i.e., the imaginary part of K/k , Fig. 10.3 revealed that chirality in addition to the lossy dielectric property gave the largest attenuation which could be as high as hundred times that the lossy dielectric spheres at about 80 GHz (which could be verified as a strong resonance scattering due to a single chiral particle [Lakhtakia et al., 1985]). We clearly elucidated the effect of enhanced attenuation using a step by step approach. First, lossy dielectric spheres increased the attenuation compared to lossless spheres, but not very much, except at frequencies lower than 90GHz. Next, the lossless chiral spheres increased the attenuation compared to lossless nonchiral spheres; but

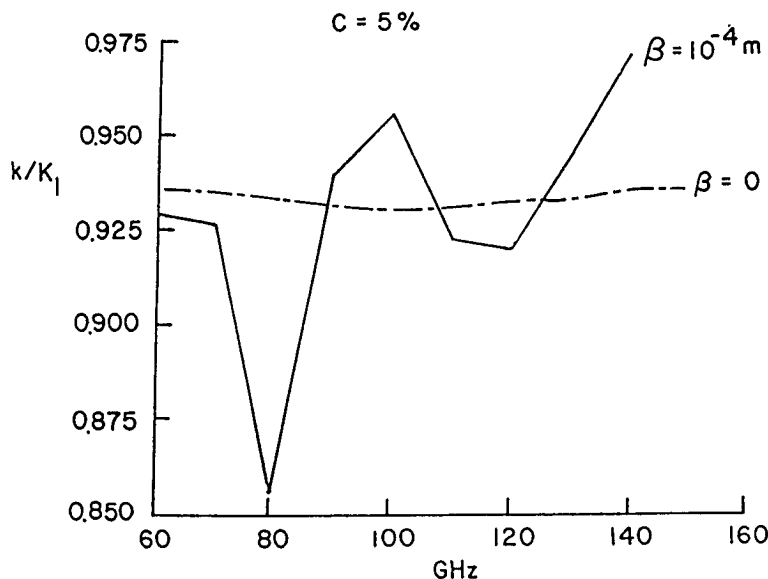


Figure 10.2 Normalized phase velocity vs. frequency for 5% chiral particles.

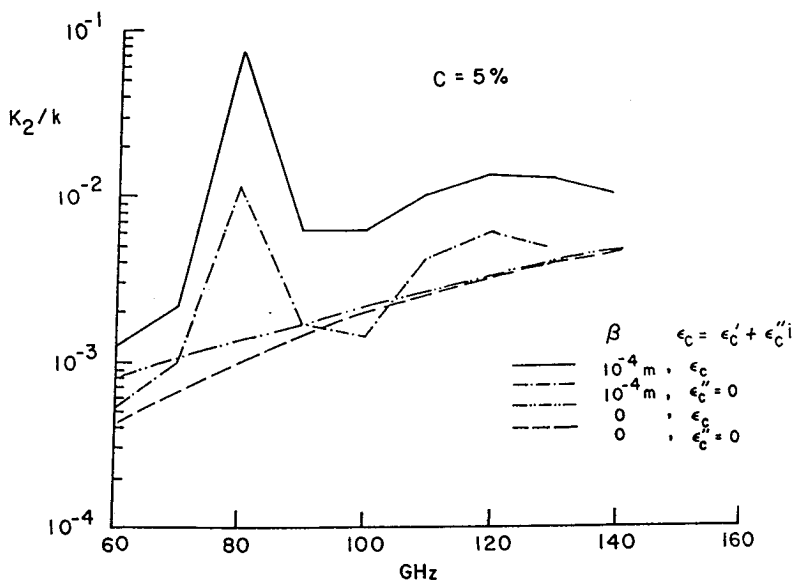


Figure 10.3 Attenuation vs. frequency for 5% chiral particles.

not always so, which could be observed in Fig. 10.3 the attempt failed in some frequency ranges. Finally, the lossy chiral spheres completed the job by achieving a constantly high attenuation in the frequency range from 60 to 140 GHz (corresponding nondimensional frequency ka was in the range of 0.25 to 0.75). This explains that the incorporation of chirality could serve to modify the properties of otherwise low-loss scatterers. The increased attenuation is mainly from the enhanced absorption due to chirality [Lakhtakia et al., 1985].

Acknowledgments

This research was supported by the Research Center for the Engineering of Electronic and Acoustic Materials at the Pennsylvania State University. The authors are grateful to Akhlesh Lakhtakia for help with the single scattering problem.

References

- [1] Barber, P. W., and C. Yeh, "Scattering of electromagnetic waves by arbitrarily shaped bodies," *Appl. Opt.*, **14**, 2864, 1975.
- [2] Barker, J. A., and D. Henderson, "Monte Carlo values for the radial distribution function of a system of fluid hard spheres," *Mol. Phys.*, **21**, 187, 1971.
- [3] Bohren, C. F., "Light scattering by an optically active spheres," *Chem. Phys. Lett.*, **29**, 458, 1974.
- [4] Jaggard, D. L., A. R. Mickelson, and C. H. Papas, "On electromagnetic waves in chiral media," *Appl. Phys.*, **18**, 211, 1979.
- [5] Khebir, A., "Low frequency approximations for the effective properties of chiral composites," *M.S. Thesis*, Pennsylvania State University, University Park, Pennsylvania, 1986.
- [6] Lakhtakia, A., V. K. Varadan, and V. V. Varadan, "Scattering and absorption characteristics of lossy dielectric, chiral, nonspherical objects," *Appl. Opt.*, **24**, 4146, 1985.

- [7] Lax, M., "Multiple scattering of waves, II, effective field in dense systems," *Phys. Rev.*, **85**, 621, 1952.
- [8] Morse, P. M., and H. Feshbach, *Methods of Theoretical Physics*, Vol. 2, McGraw-Hill, New York, 1953.
- [9] Post, E. J., *Formal Structure of Electromagnetics*, North-Holland, Amsterdam, 1962.
- [10] Tsang, L., J. A. Kong, and R. T. Shin, *Theory of Microwave Remote Sensing*, John Wiley and Sons, Inc., New York, 1985.
- [11] Varadan, V. K., V. N. Bringi, and V. V. Varadan, "Coherent electromagnetic wave propagation through randomly distributed dielectric scatterers," *Phys. Rev. D*, **19**, 2480, 1979.
- [12] Varadan, V. K., and V. V. Varadan, (eds.) *Acoustic, Electromagnetic and Elastic Wave Scattering: Focus on the T-Matrix Approach*, Pergamon, New York, 1980.
- [13] Varadan, V. K., V. N. Bringi, V. V. Varadan, and A. Ishimaru, "Multiple scattering theory for waves in discrete random media and comparison with experiments," *Radio Science*, **18**, 321, 1983.
- [14] Varadan, V. K., V. V. Varadan, and A. Lakhtakia, "On the possibility of designing anti-reflection coatings using chiral composites," *J. Wave-Material Interaction*, **2**, 71, 1987.
- [15] Varadan, V. V., Y. Ma, and V. K. Varadan, "Anisotropic dielectric properties of media containing aligned nonspherical scatterers," *IEEE Trans. Antennas Propag.*, **AP-33**, 886, 1985.
- [16] Varadan, V. V., Y. Ma, V. K. Varadan, "Propagator model including multipole fields for discrete random media," *J. Opt. Soc. Am.*, **A2**, 2195, 1985.
- [17] Varadan, V. V., A. Lakhtakia, and V. K. Varadan, "Comments on recent criticism of the T-matrix method," *J. Acoust. Soc. Am.*, **84**, 2280, 1988.
- [18] Ward, L., *The Optical Constants of Bulk Materials and Films*, Adam Hilger, Bristol, 1988.
- [19] Waterman, P. C., "Scattering by dielectric obstacles," *Alta Freq.*, **38**, (Speciale), 348, 1969.